ACS OMEGA

Open Access

http://pubs.acs.org/journal/acsodf

Article

Halogenated Phenylpyridines Possessing Chemo-Selectivity for Diverse Molecular Architectures

Nathan J. Weeks,* Lynsey K. Geray, Mikhail B. Lachapelle, and Scott T. Iacono*

Cite This: *ACS Omega* 2024, 9, 28961−28968

Read Online

ACCESS | Metrics & More | Article Recommendations | Supporting Information

ABSTRACT: Pentafluoropyridine was used as a molecular building block for the installation of aryl bromides, affording a series of multisubstituted halogenated arenes. This operationally simplistic methodology offers precise regioselectivity, ease of scalability, and high purity. ^{19}F Nuclear magnetic resonance (NMR) served as a key diagnostic tool for structural characterization, given the sensitivity with various aryl bromine substitutions on the fluorinated pyridine ring. Furthermore, molecular modeling simulations offered insight into this new class of halogenated phenylpyridines and their unique electronic and reactive properties. This study also demonstrates examples of efficient chemo-selectivity upon either metal-catalyzed aryl−aryl coupling or nucleophilic aromatic substitution of the aryl bromide or fluorinated pyridine scaffold, respectively. A diverse pool of polyarylene structures with high degree of complexity, functionalized linear polymers, and controlled network architectures were achieved from this simple methodology.

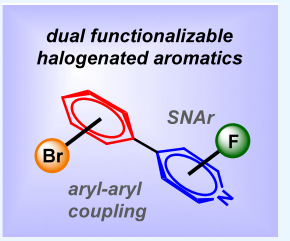

INTRODUCTION

Pentafluoropyridine (PFP) possesses the ability to undergo both multiple chemo- and regioselective addition of nucleophiles via facile nucleophilic aromatic substitution (S_NAr) to access functionalized materials for diverse applications including but not limited to recent advances in biomass quantification,[1] pharmaceuticals,[2] modified peptides,[3] cancer therapeutics,[4] organo-pollutant absorbents,[5] enhanced electrolyte cycle-life,[6] and fluoroelastomers for high cryogenic applications.[7] In addition, a comprehensive review of PFP and its utility as a highly adaptable intermediate for complex polymer architectures and their applications has recently been reported.[8] Furthermore, due to its unique electronic fluorinated heteroaromatic configuration that has been thoroughly modeled,[9−11] PFP has been utilized as an intermediate for highly efficient, regioselective transformations for fluorination,[12] deoxyfluorination,[13] dearylation,[14] hydrodefluorination,[15] and halogen exchange[16] in addition to a useful phenol protecting−deprotecting group.[17]

Of the vast examples of S_NAr chemistry reported to date, *O*- and *N*-nucleophiles, including both alkyl and aromatic constituents, are the most common for accessing multifunctional compounds given the operationally simple, mild reaction conditions with predicable substitution patterns on the 2,4,6-PFP positions.[18] On the other hand, *C*-nucleophile additions by way of generating air- and moisture-sensitive magnesium, sodium, or lithium salts from alkyl/aryl halides are less common. Work by Chambers et al. has reported one of the most comprehensive studies with *C*-nucleophile addition-substitutions using PFP demonstrating, in some cases, unique substitution patterns not otherwise observed with *O*-, *S*-, and *N*-nucleophiles.[19] This work was further supported with studies reporting *C*-nucleophile additions using cyclopropane anion salts of Mg that showed exclusive regioselective addition to the 4-position of PFP while $Zn(c\text{-}C_3H_5)_2$ and $Li(c\text{-}C_3H_5)$ afforded a distribution of 2- or 4-substituted PFP.[20] In addition, $Li(c\text{-}C_3H_5)$ also produced 2,4-substituted PFP on the heterofluoroaromatic ring limiting substrate diversity with *C*-nucelophiles. Other examples of high yielding, diverse *C*-nucleophile additions have included aryl/alkyl Grignard reagents,[21] alkyl transfer from phosphonium ylides,[22] and via mild tetramethylsilylacetylene deprotection[23] all with regio-controlled substitution limited to the PFP 4-position. A final example showed the ability to install PFP on the side chain of poly(4-phenyllithium)styrene, which is the only reported use of *C*-nucleophile additions related to chain-extended macromolecular systems.[24]

A logical alternative to achieving carbon−carbon connections with PFP would be utilizing metal-mediated coupling, and yet surprisingly, only limited reports on this strategy have been reported and are illustrated in Scheme 1. A significant advancement in this capacity reported by Qin et al. have demonstrated PFP can be directly coupled to a diverse pool of donor−acceptor aryl bromides or triflates via dual photoredox Ir−Pd-catalyzed cross-coupling in very good isolated yields (route a).[25] In this work, attempted couplings with other fluoroaromatics, specifically hexafluorobenze, failed to achieve the desired coupled adduct and only a single report by Gutov

Received: April 24, 2024
Revised: June 4, 2024
Accepted: June 12, 2024
Published: June 18, 2024

Scheme 1. Previous Examples Utilizing Different Methodologies for the Preparation of Alkyne/Aryl Pd-Mediated Coupling to Halogenated Pyridines

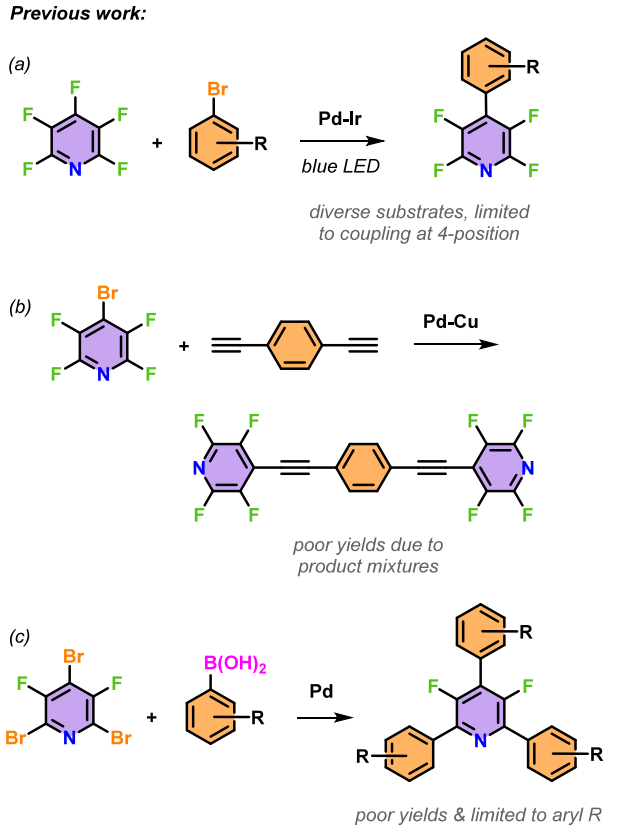

Scheme 2. Current Work on the Synthesis of Multihalogenated Pyridines and New Routes toward Multifunctional Compounds

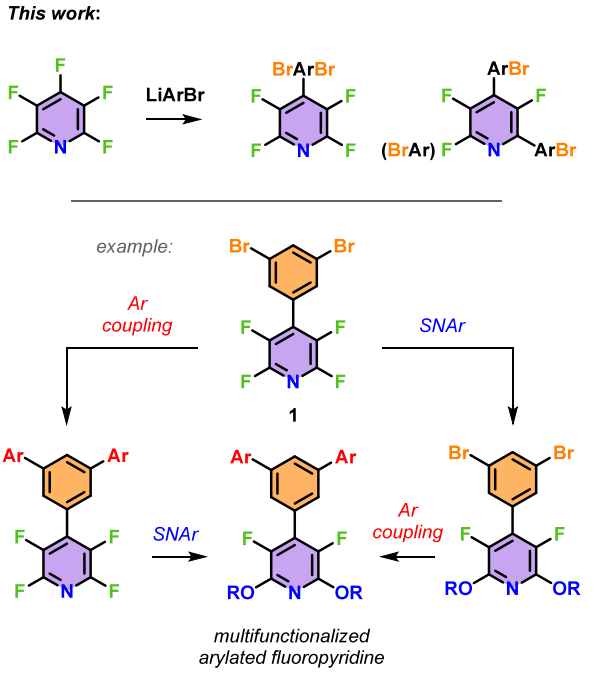

et al. has demonstrated the coupling of PFP affording perfluoro-4,4′-bipyridine (route b).[26] Either methodology is limited to PFP 4-substitution, which confines the ability to access multifunctional substrates or polymeric systems. A more conventional route toward *C*-substituted fluoropyridine entailed Pd-catalyzed cross-coupling 4-bromo-2,3,5,6-tetrafluoorpyridine and diphenylaceteylene or 2,4,6-tribromo-3,5-difluoropyridine with phenylboronic acids via Sonogashira or Suzuki coupling conditions, respectively (route c).[27,28]

These aforementioned accounts require modification of PFP with aryl bromides, which is limited to substitution at the 4- or 2,4,6-position and reports modest to poor isolated yields. Therefore, there remains a need to develop a methodology for *C*-nucleophile addition to PFP in order to afford regioselective, multihalogentated aromatic intermediates that can be tailored for further functionalization utilizing commonly practiced aryl−aryl coupling of the aryl bromides as well as the ability to further modify the appended fluoroheteroaromatic via facile S_NAr transformations. In this account, as outlined in Scheme 2, we demonstrate controlled, high-yielding bromoaryllithium additions to PFP affording a series of multifunctional aryl bromides appended to fluorinated pyridine at various specific positions with high regioselectivity. This account will further detail how the installed π-conjugated heterofluoroaromatic units affect the electronic properties of these aryl bromide systems as it relates to their regio-controlled architecture in addition to demonstrating several examples of chemo-selective aryl−aryl coupling with subsequent S_NAr chemistry by the use of phenolic nucleophiles in order to obtain compounds with high complexity. An example is illustrated in Scheme 2 (lower caption) whereby 4-(3,5-dibromophenyl)-2,3,5,6-tetrafluoropyridine (**1**) is used as an example demonstrating that the preparation of a multifunctionalized arylated fluoropyridine can be achieved from two discrete chemoselective transformational pathways without compromising the functionality of the nonreacting unit. This ability to rapidly access such complex building blocks via facile transformations would be of interest for a broader scope of agrochemicals, materials possessing controlled architectures, or polymeric systems.

RESULTS AND DISCUSSION

Methodology Optimization. The preparation of aryl bromide functionalized fluorinated pyridines, specifically 4-(3,5-dibromophenyl)-2,3,5,6-tetrafluoropyridine (**1**), 2,4-bis-(4-bromophenyl)-3,5,6-trifluoropyridine (**2**), and 2,4-bis(4-bromophenyl)-3,5,5-trifluoropyridine (**3**), was achieved by bromine−lithium exchange using *tert*-butyl lithium and 1,4-dibromobenzene or 1,3,6-tribromobenzne generating lithiated aryl bromide intermediates **I** and **II** in situ that underwent nucleophilic aromatic substitution (S_NAr) with pentafluoropyridine (PFP) (Scheme 3). In order to minimize side reactions typical of halogen-metal exchange that often include dilithiation ($ArLi_2$) and/or aryl coupling (Br−Ar−Ar−Br), the reactions were carefully monitored by GCMS, maintained at −78 °C with high dilution, and PFP added neat in a single portion. Optimized conditions after adjusting for time, temperature, solvent, and *tert*-butyl lithium stoichiometry afforded **1**−**3** in scalable 5 g quantities in excellent isolated yields for **1** and **2** (>95%) and modest yield for **3** (>50%) due to insolubility in diethyl ether. For the preparation of the desired 4-substituted **1**, the minor 2-substituted isomer was unavoidable after various attempts and was also not possible to separate from the product mixture by chromatography or recrystallization. Based on ^{19}F NMR of the product mixture, less than 5% of the 2-isomer of **1** was formed as the

https://doi.org/10.1021/acsomega.4c03945
ACS Omega 2024, 9, 28961−28968

Scheme 3. Synthesis of Monomers 1−2 and 3 from PFP upon Addition of Organolithium Intermediates I and II, Respectively[a]

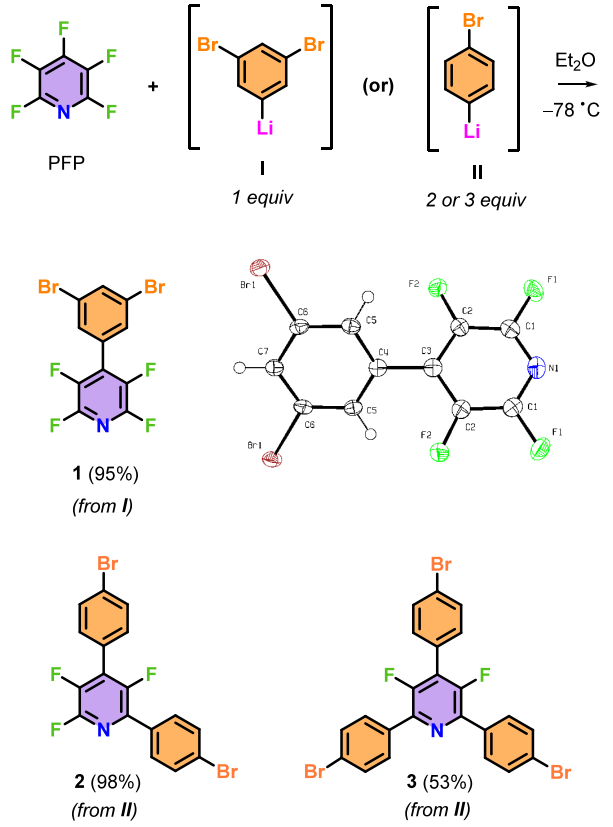

[a]Inset includes atom-labeled ORTEP representation of **1**; thermal ellipsoids shown at 50% probability.

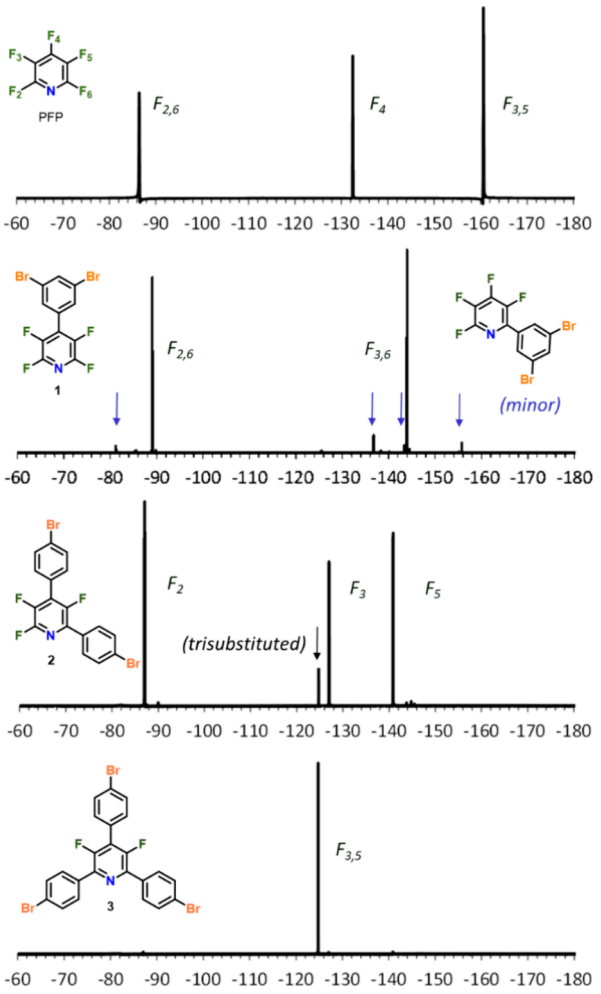

Figure 1. ^{19}F NMR overlay of compounds **1**-**3** in $CDCl_3$.

thermodynamically preferred adduct. In addition, the preparation of **2** was achieved with a minor component of **3** (3%) due to the over addition of lithiated aryl bromide intermediate **I**. While both compounds **1** and **2** possess minor constituents, they are considered acceptable for reagent grade transformations (>95% purity) and remain purposeful for the remainder of this study.

Structural Characterization. Arylated fluoropyridines **1**−**3** were structurally characterized by multinuclear NMR and purity determined by GCMS. Specifically, ^{19}F NMR served as a key diagnostic tool for reaction monitoring as well as purity given the nuclei's broad magnetic chemical shift and sensitivity to electronic, steric, and inductive effects of substitution. Figure 1 shows the overlay of PFP as it undergoes aryl bromide substitution at various positions. With compound **1**, the chemical conversion of PFP (with multiplets at midpoint for clarity) at −87 ($F_{2,6}$), −130 (F_4), and −161 ppm ($F_{3,5}$) with a relative integration ratio of 2:1:2 affords two sets of chemical shifts at −88 ($F_{2,6}$) and −143.8 ppm ($F_{3,5}$) of equal intensity. The minor 2-substituted isomer is also shown and detailed more in Figure S1. Compound **2** desymmeterizes the fluorinated pyridine affording shifts at −87 ppm (F_2), −127 ppm (F_3), and −1140 ppm (F_5) in 1:1:1 integration ratio with a trace amount of trisubstituted compound **3**. Finally, compound **3** reveals a single chemical shift at −125 ppm whereby the equivalent fluorines at either the 3- or 5-position of the pyridine ring remain unreacted due to poor charge polarization of the C−F rendering these positions inert to most S_NAr chemistry.[18]

Molecular Orbital Simulations. In order to understand the influence of electron delocalization of arylated fluorinated pyridines **1**−**3**, surrogates **A**−**C** were modeled by computational simulations as shown in Figure 2. For structure **A**, the HOMO appears to attain high delocalization of electron density on the aromatic ring, while the LUMO configuration produces nearly uniform delocalization of electron density among both the aryl and 2,3,5,6-tetrafluoropyrine π-orbitals. In the case with structure **A**, the HOMO depicts 2,6-fluoropyridine positions vacant of electron density and suitable for S_NAr substitution, as demonstrated in the subsequent section of this work. These HOMO−LUMO observations correlate with a recent study whereby the fluoropyridine undergoes ring and C−F bond contractions due to fluorine's unique ability to donate election density from its σ-orbitals.[31] For models **B** and **C**, HOMO representations show electron delocalization on the 2- and 2,6-pyridine positions, respectively, leaving the 4-position entirely unoccupied. Contrastingly, the LUMOs of **B** and **C** appear to generate electron density across the entire molecules similar to structure **A** with slightly higher electron density in the 4-position. These observations suggest that the fluoropyridine moiety facilitates favorable electron delocalization suitable for extended π−π conjugated systems and potential for symmetry-influenced, tunable electronic band gaps. The electrostatic potential (ESP)

https://doi.org/10.1021/acsomega.4c03945
ACS Omega 2024, 9, 28961−28968

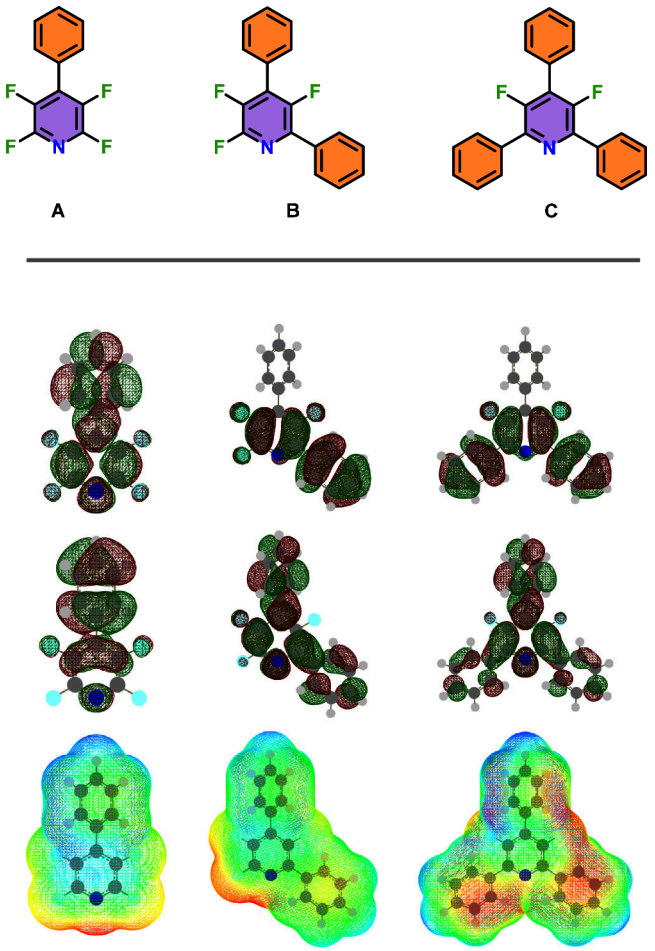

Figure 2. Molecular orbital diagrams of HOMOs (top row) and LUMOs (middle row) and ESP mapped total electron density isosurfaces (bottom row) of compounds **A**−**C**. Electronic structure calculations were performed using Gaussian 09 with the DFT B3LYP functional and 6-311g+(2d,p) basis set.

maps of model structures **A** and **B** show that the majority of the electronegativity is generated at the location of nitrogen lone pairs and C−F σ-bond(s). In the case for model **C**, the electronegativity is distributed uniformly on the aromatic rings, suggesting that the 3,5-fluoropyrine ring, as a unit, undergoes extended delocalization.

Substrate Compatibility with Halogen Selectivity. In order to demonstrate substrate compatibility of aryl bromide, fluoropyridine compounds (**1**−**3**) underwent a series of Pd-catalyzed aryl−aryl coupling and S_NAr substitution reactions in order to demonstrate halogen selectivity as illustrated in Figure 3. It is important to note that while S_NAr substitution with, for example, PFP has been commonly accepted, recent reports have shown that nucleophilic addition to fluorinated pyridine undergoes a concerted mechanism[29,30] due to its fluoroaromatic nature rather than the commonly accepted stepwise mechanism.[31] In the first example, aryl-coupled adduct **1a** was prepared from **1** using Pd coupling with two equivalents of phenyl boronic acid in overall good isolated yields (88%) while demonstrating that the tetrafluoropyridine (TFP) moiety remained intact as observed by ^{19}F NMR analysis. This demonstrated the capacity to adopt from a plethora of common transition metal-mediated transformations in order to prepare polyarylene systems that can be either pre- or postfunctionalized using the pendant TFP moiety via S_NAr substitution. Polymerization of **1** with hydroquinone using facile S_NAr substitution conditions adapted from recent protocols[32] afforded **P1** as a transparent, film forming linear aryl ether system with a number-average molecular weight (by ^1H NMR end group analysis) of 16,000 g mol^{-1} with no observed competing S_NAr substitution of the aryl bromides. The glass-transition temperature (T_g) and onset of thermal decomposition in nitrogen (T_d) of **P1** yielded 123 and 455 °C, respectively, which is comparable to commercial high-performance poly(arylether)s. Furthermore, this fluoropyrdine aryl ether polymer can be adapted to other combinations of aryl and/or alkyl bis-nucleophiles with varying molecular weight and can undergo further postfunctionalization with metal-mediated coupling with the labile aryl bromides. Furthermore, the ability to preinstall molecular functional groups onto **1** was successfully attempted by reacting with two equivalents of phenol affording **1b**, which exhibits no reactivity toward the 3,5-dibromophenyl units. Similarly, compound **2** underwent S_NAr substitution at the 6-position of the 3,5,6-trifluoropyridine core with phenol in overall good isolated yield affording **2a**. This allows the ability to react the intact aryl bromides with additional reactive species amenable to metal-mediated couplings, as similarly discussed for the preparation of **1a**. Lastly, a controlled network (**N3**) was prepared by Pd-catalyzed coupling of **3** with diphenylboronic acid affording an insoluble network that demonstrated a T_d onset of 500 °C and pyrolysis to glass char (5%) at 616 °C in nitrogen. Given the thermal stability of **N3**, it is conclusive that the 3,5-difluoropyridine unit remains intact during the aryl−aryl coupling conditions and possessing a potential value as a high temperature resistant hole-transport core structure when coupled with π-donor motifs.

CONCLUSIONS

This study has demonstrated a methodology utilizing pentafluoropyridine a simple molecular building block toward regioselective installation of aryl bromides via organolithium chemistry affording a series of multisubstituted halogenated arenes as synthetic intermediates. Because of their unique selective reactivity as supported by molecular modeling simulations, this work demonstrated examples of efficient chemo-selectivity upon either metal-catalyzed aryl−aryl coupling of the aryl bromide or S_NAr using any combination of aryl/alkyl *O*-, *S*-, *N*-, and *C*-nucleophiles of the fluorinated pyridine scaffold. As such, a diverse pool of polyarylene structures with high degree of complexity by variation of Pd-catalyzed cross coupling or S_NAr substitution could be achieved for small-molecule libraries directed toward agrochemicals, pharmaceuticals, as well as other targets of synthetic interest. In addition, this methodology can be extended into designing monomers for functionalized linear polymers with vary architectures or cross-linked systems either by conventional step- or chain-growth pathways.

EXPERIMENTAL SECTION

General Methods. All chemicals and solvents were obtained from commercial sources as reagent-grade or used as received. Flasks and syringes were flame-dried under a vacuum and allowed to cool in a desiccator prior to use. All reactions and solvent transfers were flushed and carried out under an atmosphere of argon.

https://doi.org/10.1021/acsomega.4c03945
ACS Omega 2024, 9, 28961−28968

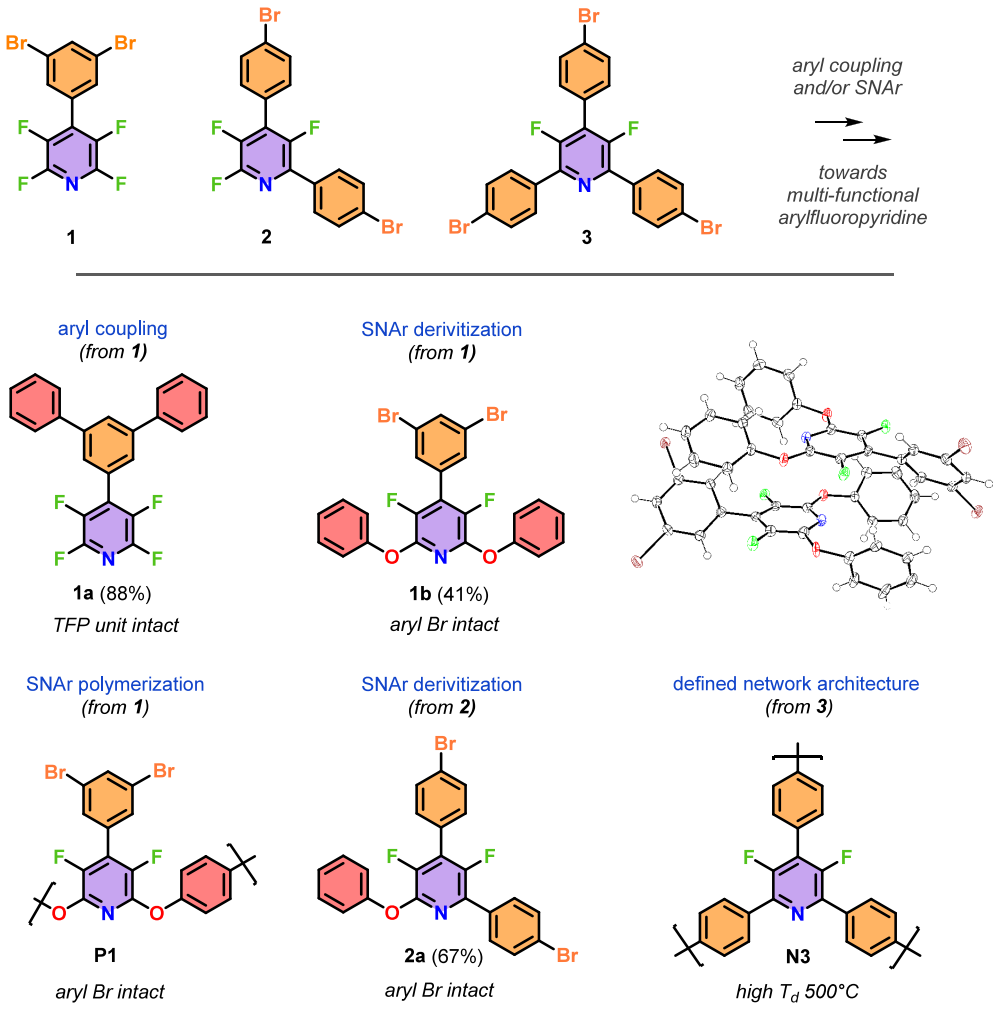

Figure 3. Selected examples of adaptable Pd aryl−aryl coupling or S_NAr substitution with bromoarylfluoropyridine compounds **1**−**3**. Inset includes ORTEP representation of **1b**; ellipsoids shown at 50% probability, and only the major component of disorder at one phenyl ring is shown (atom labels: O-red; N-blue; F-green; Br-brown).

Instrumentation. ^{1}H, ^{13}C, and ^{19}F NMR spectra were recorded on a Jeol 500 MHz spectrometer. Chemical shifts were reported in parts per million (ppm), and the residual solvent peak was used as an internal reference: proton (chloroform δ 7.26), carbon (chloroform, C{D} triplet, δ 77.0 ppm), and fluorine ($CFCl_3$ δ 0.00) were used as a reference. Data are reported as follows: chemical shift, multiplicity (s = singlet, d = doublet, t = triplet, m = multiplet with reported range or at midpoint), coupling constants (Hz), and integration.

Gas chromatography-mass spectrometry (GC-MS) analyses were performed on an Agilent 7890 gas chromatograph coupled to an Agilent 5975C electron impact mass spectrometer with a temperature gradient of 80−250 °C at 15 °C/min after an initial 2 min temperature hold at 80 °C.

Differential scanning calorimetry (DSC) analyses were performed on a TA 2500 DSC instrument utilizing aluminum hermetic pans. Melting temperature (M_p) or glass-transition temperature (T_g) analyses were carried out using a 5 °C/min temperature gradient under nitrogen and reported at T_{max} or at midpoint/half height (third scan) using graphical software, respectively. Thermogravimetric analyses (TGA) were performed on a TA 5500 utilizing platinum pans at a 10 °C/min temperature gradient under nitrogen. Simultaneous thermodynamic (SDT) analysis were performed on a TA 650 utilizing ceramic pans at 10 °C/min temperature gradient under nitrogen.

Single crystal X-ray diffraction studies were carried out on a Rigaku XtaLAB synergy, Dualflex, HyPix3000 diffractometer equipped with a Cu Kα radiation source (λ = 1.542 Å). Suitable crystals were selected and mounted on a Cryoloop secured with a Paratone-N oil. The crystal of interest was kept at a steady T of 100.0(3) K in a nitrogen gas stream during data collection. A crystal-to-detector distance was 40.6 mm using an exposure time of 0.2 s with a scan width of 0.50° for all crystals in this work. X-ray quality crystals of **1** and **1b** were obtain by slow evaporation of chloroform.

The data collection routine, unit cell refinement, and data processing were carried out with the program CrysAlisPro (version 43.91a) and scaled using an empirical absorption correction implemented in the SCALE 3 ABSPACK software program, as well as a numerical absorption correction based on Gaussian integration over a multifaceted crystal model. The structure was solved using ShelXT 2018/2[33] and refined using ShelXL 2019/3[34] by least-squares minimization via Olex2.[35] The final refinement model involved anisotropic displacement parameters for nonhydrogen atoms and a riding model for all

https://doi.org/10.1021/acsomega.4c03945
ACS Omega 2024, 9, 28961−28968

hydrogen atoms. Olex2, Mercury, and ORTEP3 were used for molecular graphics generation.

Computational Modeling and Simulation. All models for this work were computed using the Gaussian 09W suite of programs, including the use of Gaussview 5 to generate three-dimensional figures. Each molecule to be modeled was constructed in Chem3D 21.0.0 and had its geometry optimized first with the molecular mechanics geometry optimization feature included in the suite. These structures were then used as starting structures for optimization by using the B3LYP density functional and the 6-311g+(2d,p) basis set for all atoms. Geometries optimized with DFT were verified with frequency analysis at the same level of theory as the optimization to ensure no imaginary vibrational frequencies. Orbital population analysis was also conducted at the same level of theory.

*General Procedure for Preparation of Compounds **1**–**3**.* For a 5 g product scale, *tert*-butyllithium (1.2 equiv., 1.7 *M* in pentane) was added dropwise via syringe to either tribromobenzene (1 equiv for **1**) or 1,4-dibromobenzene (2 equiv for **2**, 3 equiv for **3**) in Et_2O at −78 °C. The bromo-lithium exchange was monitored by GCMS until the aryl bromide was consumed (typically after 30 min). Pentafluoropyridine (1.2 equiv for **1**, 2.2 equiv for **2**, and 3.4 equiv for **3**) was then added portion wise via syringe, and the reaction was allowed to warm to room temperature. After 16 h, the reaction is quenched with saturated ammonium chloride (1 × 100 mL), extracted with diethyl ether (3 × 30 mL), and washed with deionized water (1 × 100 mL) and saturated brine (1 × 100 mL). The combined organic layers were dried with magnesium sulfate, vacuum filtered, concentrated using a rotary evaporator, and placed under a high vacuum.

*4-(3,5-Dibromophenyl)-2,3,5,6-tetrafluoropyridine (**1**).* Compound **1** was purified by dissolving in minimal amount of absolute ethanol followed by precipitation from deionized water, vacuum filtered, and dried in vacuum oven at 65 °C affording a white solid (95%). M_p 112 °C. ^{1}H NMR ($CDCl_3$, 500 MHz) δ 7.83 (s, 1H), 7.60 (s, 2H); $^{13}C\{^1H\}$ NMR (126 MHz) δ 144.5 (dm, J = 249 Hz), 138.5 (dm, J = 250 Hz), 136.2, 135.8, 131.3, 130.5−130.1 (m) 123.5; ^{19}F NMR ($CDCl_3$, 471 MHz) δ −88.1−(−89.0) (m, 2F), −143.7−(−143.9) (m, 2F); GC−EIMS (70 eV) m/z (% relative intensity) 384 ($[M]^+$, 90), 225 (100), 175 (20), 74 (15).

*2,4-Bis(4-bromophenyl)-3,5,6-trifluoropyridine (**2**).* Compound **2** was recrystallized from hot absolute ethanol and vacuum filtered under high vacuum affording a white solid (98%). M_p 125 °C. ^{1}H NMR ($CDCl_3$, 500 MHz) δ 7.82 (d, J = 6.50, 2H), 7.66 (d, J = 7.49 Hz, 2H), 7.61 (d, J = 7.50, 2H), 7.41 (d, J = 6.50, 2H); $^{13}C\{^1H\}$ NMR (126 MHz) δ 154.0−138.0 (unresolved multicity due to C−F coupling), 132.5, 131.9, 130.4, 125.8, 124.9, 124.4; ^{19}F NMR ($CDCl_3$, 471 MHz) δ −86.9−(−87.1) (m, 1F), −126.9−(−127.0) (m, 1F), −140.0−(−140.8) (m, 1F); GC−EIMS (70 eV) m/z (% relative intensity) 443 ($[M]^+$, 100), 282 (10), 263 (10).

*2,4,6-Tris(4-bromophenyl)-3,5-difluoropyridine (**3**).* Compound **3** was recrystallized from hot absolute ethanol and vacuum filtered under high vacuum affording a white solid (53%). M_p maxima at 125 and 130 °C. ^{1}H NMR ($CDCl_3$, 500 MHz) δ 7.90 (d, J = 8.51 Hz, 4H), 7.67 (d, J = 8.5 Hz, 2H), 7.62 (d, J = 8.51, 4H), 7.42 (d, J = 8.0 Hz, 2H); $^{13}C\{^1H\}$ NMR (126 MHz) δ 153.8, 151.7, 141.8 (unresolved multiplicity), 133.8, 132.0, 131.8, 131.7, 130.4, 126.2, 124.2, 124.0; ^{19}F NMR ($CDCl_3$, 471 MHz) δ −124.7 (2F); GC−EIMS (70 eV) m/z (% relative intensity) 580 ($[M]^+$, 100), 500 (15), 420 (15), 339 (15), 319 (15), 238 (20), 207 (15).

*4-([1,1′:3′,1″-Terphenyl]-5′-yl)-2,3,5,6-tetrafluoropyridine (**1a**).* Compound **1** (196 mg, 0.51 mmol), phenylboronic acid (155 mg, 1.27 mmol), sodium carbonate (4 mL, 2 *M* aqueous solution), and palladium tetrakis(triphenylphosphine) (29.6 mg, 0.019 mmol) were combined in dimethylformamide (20 mL) and allowed to stir at 80 °C for 48 h at room temperature. The reaction was monitored by GCMS until 100% conversion of the desired product is observed. The solution was vacuum filtered to remove suspended solids and washed with dichloromethane (50 mL). The filtrate was combined with saturated ammonium chloride (100 mL), and the aqueous layer was extracted with diethyl ether (2 × 50 mL). The combined organic fractions were washed with saturated brine (1 × 100 mL), dried with magnesium sulfate, vacuum filtered over a dual plug of silica/Celite, concentrated using rotary evaporation, and dried under high vacuum affording a white solid (169 mg, 88%). ^{1}H NMR ($CDCl_3$, 500 MHz) δ 7.94 (br s, 1H), 7.70−7.65 (m, 6H), 7.51−7.40 (m, 6H); $^{13}C\{^1H\}$ NMR (126 MHz) δ 145.3 (dm, J = 249 Hz), 142.8, 140.0, 139.4 (dm, J = 252 Hz), 133.5−133.2 (m), 129.1, 128.3, 128.2, 127.3; ^{19}F NMR ($CDCl_3$, 471 MHz) δ −90.2−(−91.1) (m, 2F), −144.1−(−144.4) (m, 2F); GC−EIMS (70 eV) m/z (% relative intensity) 379 ($[M]^+$, 100), 77 (50), 51 (40).

*4-(3,5-Dibromophenyl)-3,5-difluoro-2,6-diphenoxypyridine (**1b**).* 4-(3,5-Dibromophenyl)-2,3,5,6-tetrafluoropyridine (**1**) (750 mg, 1.95 mmol), phenol (367 mg, 3.99 mmol), and cesium carbonate (1.30 g, 3.99 mmol) were suspended in DMF (30 mL) at room temperature. The reaction was monitored by GCMS until 100% conversion of the desired product is observed. After 16 h, the solution was vacuum filtered to remove suspended solids and washed with dichloromethane (30 mL). The filtrate was combined with saturated ammonium chloride (100 mL), and the aqueous layer was extracted with DCM (2 × 50 mL). The combined organic fractions were washed with saturated brine (1 × 100 mL), dried with magnesium sulfate, vacuum filtered over a dual plug of silica/Celite, concentrated using rotary evaporation, and dried under high vacuum affording a white solid (423 mg, 41%). ^{1}H NMR ($CDCl_3$, 500 MHz) δ 7.80 (br s, 1H), 7.67 (br s, 2H), 7.27−7.24 (m, 4H), 7.13−7.10 (m, 2H), 7.05−7.03 (m, 4H); $^{13}C\{^1H\}$ NMR (126 MHz) δ 153.5, 144.4−144.3 (m), 140.0, 138.3, 135.4 (m), 131.7, 130.7, 129.3, 124.8, 123.2, 120.6; ^{19}F NMR ($CDCl_3$, 471 MHz) δ −146.0 (s, 2F), −144.1−(−144.4) (m, 2F); GC−EIMS (70 eV) m/z (% relative intensity) 533 ($[M]^+$, 70), 309 (50), 77 (100), 51 (55).

*Polymer (**P1**).* 4-(3,5-Dibromophenyl)-2,3,5,6-tetrafluoropyridine (**1**) (500 mg, 1.30 mmol), hydroquinone (143 mg, 1.30 mmol), and cesium carbonate (889 mg, 2.72 mmol) were suspended in DMF (100 mL) at 50 °C. After 24 h, the solution was poured into rigorously stirred water (250 mL) at 0 °C, and the suspended solid was vacuum filtered, washed with MeOH (3 × 50 mL), and dried in a vacuum oven at 60 °C for 24 h, affording a tan powder (450 mg). ^{1}H NMR ($CDCl_3$, 500 MHz) δ 9.30 (br s, 1H, − OH end-group), 8.15−7.50 (br m, Ar−H), 7.30−6.50 (br m, Ar−H).

*2,4-Bis(4-bromophenyl)-3,5-difluoro-6-phenoxypyridine (**2a**).* 2,4-Bis(4-bromophenyl)-3,5,6-trifluoropyridine (**2**) (500 mg, 1.129 mmol), phenol (112 mg, 1.85 mmol), and cesium carbonate (405 mg, 1.24 mmol) were suspended in DMF (20 mL) at room temperature. The reaction was monitored by

https://doi.org/10.1021/acsomega.4c03945
ACS Omega 2024, 9, 28961−28968

GCMS until 100% conversion of the desired product is observed. After 16 h, the solution was vacuum filtered to remove suspended solids and washed with dichloromethane (50 mL). The filtrate was combined with saturated ammonium chloride (100 mL), and the aqueous layer was extracted with diethyl ether (2 × 50 mL). The combined organic fractions were washed with saturated brine (1 × 100 mL), dried with magnesium sulfate, vacuum filtered over a dual plug of silica/Celite, concentrated using rotary evaporation, and dried under high vacuum affording a yellow solid (389 mg, 67%). ^{1}H NMR ($CDCl_3$, 500 MHz) δ 7.90−7.88 (m, 2H), 7.63−7.61 (m, 2H), 7.56−7.53 (m, 2H), 7.33−7.31 (m, 2H), 7.27−7.24 (m, 2H), 7.06−7.03, (m, 1H), 6.82−6.81 (m 2H); ^{13}C{^{1}H} NMR (126 MHz) δ 157.2, 152.8 (m), 150.9 (m), 137.4 (m), 135.8 (m), 133.8 (m), 132.6 (m), 131.9, 131.8, 131.4, 130.3, 130.2, 129.9, 124.3, 124.2, 123.5, 115.5; ^{19}F NMR ($CDCl_3$, 471 MHz) δ −124.6 (m, 2F); GC−EIMS (70 eV) m/z (% relative intensity) 517 ([M]$^{+}$, 100), 359, 358 (50), 252 (20), 77 (50), 51 (20).

*Network (**N3**).* Compound **3** (0.25 mmol, 1 equiv), 1,4-benzenedibornic acid (0.25 mmol, 1 equiv), sodium carbonate (3 mL, 2 M aqueous solution), and palladium tetrakistriphenylphosphine (0.0125 mmol, 0.05 equiv) were combined with dimethylformamide (15 mL) at 80 °C for 24 h. The solution was suspended in deionized water (100 mL), vacuum filtered to remove suspended solids, and washed with methanol (3 × 50 mL). The filtrate was dried in a vacuum oven at 65 °C for 24 h, affording an off-white solid powder (90% by weight recovery).

■ ASSOCIATED CONTENT

Supporting Information

The Supporting Information is available free of charge at https://pubs.acs.org/doi/10.1021/acsomega.4c03945.

^{1}H, ^{19}F, ^{13}C, and GCMS for compounds **1**−**3**, **1a**, **1b**, and **2b**; ^{1}H, ^{19}F, DSC, and TGA data for **P1**; TGA data for **N3**. Supplementary crystallographic data for the single crystal X-ray structure can be obtained free of charge via www.ccdc.cam.ac.uk/data_request/cif or by emailing da-ta_request@ccdc.cam.ac.uk, or by contacting the Cambridge Crystallographic Data Centre, 12 Union Road, Cambridge CB2 1EZ, UK, fax: +44-1223-336033 with reference to CCDC 2348785 (for **1**) and 2347996 (for **1b**) (PDF)

■ AUTHOR INFORMATION

Corresponding Authors

Nathan J. Weeks − *Department of Chemistry and Chemistry Research Center, Laboratories for Advanced Materials, United States Air Force Academy, Colorado Springs, Colorado 80840, United States*; Email: nathan.weeks@afacademy.af.edu

Scott T. Iacono − *Department of Chemistry and Chemistry Research Center, Laboratories for Advanced Materials, United States Air Force Academy, Colorado Springs, Colorado 80840, United States*; orcid.org/0000-0002-2313-2618; Email: scott.iacono@afacademy.af.edu

Authors

Lynsey K. Geray − *Department of Chemistry and Chemistry Research Center, Laboratories for Advanced Materials, United States Air Force Academy, Colorado Springs, Colorado 80840, United States*

Mikhail B. Lachapelle − *Department of Chemistry and Chemistry Research Center, Laboratories for Advanced Materials, United States Air Force Academy, Colorado Springs, Colorado 80840, United States*

Complete contact information is available at: https://pubs.acs.org/10.1021/acsomega.4c03945

Notes

The authors declare no competing financial interest.

■ ACKNOWLEDGMENTS

The authors acknowledge the Air Force Office of Scientific Research (AFOSR) and the Defense Threat Reduction Agency (DTRA) for support through memorandum of agreement with the US Air Force Academy.

■ REFERENCES

(1) Kenny, J. K.; Medlin, W.; Beckham, G. T. Quantification of phenolic hydroxyl groups in lignin via ^{19}F NMR spectroscopy. *ACS Sust. Chem. & Eng.* **2023**, *11*, 5644−5655.

(2) Darehkordi, A.; Ramezani, M.; Rahmani, F.; Ramezani, M. J. Design, synthesis and evaluation of antibacterial effects of a new class of piperazinylquinolone derivatives. *Heterocycl. Chem.* **2016**, *53*, 89−94.

(3) Gimenez, D.; Mooney, C. A.; Dose, A.; Sandford, G.; Coxon, C. R.; Cobb, S. L. The application of perfluoroheteroaromatic reagents in the preparation of modified peptide systems. *Org. Biomol. Chem.* **2017**, *15*, 4086−4095.

(4) Yang, W. Y.; Breiner, B.; Kovalenko, S. V.; Ben, C.; Singh, M.; LeGrand, S. N.; Sang, Q. X. A.; Strouse, G. F.; Copland, J. A.; Alabugin, I. V. C-lysine conjugates: pH-controlled light-activated reagents for efficient double-stranded DNA cleavage with implications for cancer therapy. *J. Am. Chem. Soc.* **2009**, *131*, 11458−11470.

(5) Gomri, M.; Abderrazak, H.; Chabbah, T.; Souissi, R.; Saint-Martin, P.; Casabianca, H.; Chatti, S.; Mercier, R.; Errachid, A.; Hammami, M.; Jaffrezic-Renault, N. Adsorption characteristics of aromatic pollutants and their halogenated derivatives on bio-based poly(etherpyridine)s. *J. Environ. Chem. Eng.* **2020**, *8*, No. 104333.

(6) Zhang, X.; Liu, G.; Zhou, K.; Jiao, T.; Zou, Y.; Wu, Q.; Chen, X.; Yang, Y.; Zheng, J. Enhancing cycle life of nickel-rich Li-$Ni_{0.9}Co_{0.05}Mn_{0.05}O_2$ via a highly fluorinated electrolyte additive − pentafluoropyridine. *Energy Mater.* **2022**, *1*, 100005.

(7) Friesen, C. M.; Kelley, A. R.; Iacono, S. T. Shaken not stirred: perfluoropyridine-polyalkylether prepolymers. *Macromolecules* **2022**, *55*, 10970−10979.

(8) Gautam, R.; Geniza, I.; Iacono, S. T.; Friesen, C. M.; Jennings, A. R. Perfluoropyridine: discovery, chemistry, and applications in polymers and material science. *Molecules* **2022**, *27*, 1616.

(9) Vlasov, V. M.; Aksenov, V. V.; Rodionov, P. P.; Beregovaya, I. V.; Shchegoleva, L. N. Unusual lability of pentafluorophenoxy group in reactions of potassium aroxides with pentafluoropyridine. *Russ. J. Org. Chem.* **2002**, *38*, 115−125.

(10) Fuhrer, T. J.; Houck, M.; Corley, C. A.; Iacono, S. T. Theoretical explanation of reaction site selectivity in the addition of a phenoxy group to perfluoropyridine. *J. Phys. Chem. A* **2019**, *123*, 9450−9455.

(11) Liljenberg, M.; Brinck, T.; Rein, T.; Svensson, M. Svensson, M Beilstein Utilizing the σ-complex stability for quantifying reactivity in nucleophilic substitution of aromatic fluorides. *J. Org. Chem.* **2013**, *9*, 791−799.

(12) Murray, C. B.; Sandford, G.; Korn, S. R.; Yufit, D. S.; Howard, J. A. K. New fluoride ion reagent from pentafluoropyridine. *J. Fluor. Chem.* **2005**, *126*, 569−574.

(13) Brittain, W. D. G.; Cobb, S. L. Carboxylic acid deoxyfluorination and one-pot amide bond formation using pentafluoropyridine (PFP). *Org. Lett.* **2021**, *23*, 5793−5798.
(14) Panferova, L. I.; Zubkov, M. O.; Kosobokov, M. D.; Dilman, A. D. Light-Promoted Dearylation of Perfluorinated Aryl Sulfides with N-Heterocyclic Carbene−Borane. *Org. Lett.* **2022**, *24*, 8559−8563.
(15) Senaweera, S. M.; Singh, A.; Weaver, J. D. Photocatalytic Hydrodefluorination: Facile Access to Partially Fluorinated Aromatics. *J. Am. Chem. Soc.* **2014**, *136*, 3002−3005.
(16) Froese, R. D. J.; Whiteker, G. T.; Peterson, T. H.; Arriola, D. J.; Renga, J. M.; Shearer, J. W. Computational and Experimental Studies of Regioselective S_NAr Halide Exchange (Halex) Reactions of Pentachloropyridine. *J. Org. Chem.* **2016**, *81*, 10672−10682.
(17) Brittain, W. D. G.; Cobb, S. L. Tetrafluoropyridyl (TFP): A general phenol protecting group readily cleaved under mild conditions. *Org. Biomol. Chem.* **2019**, *17*, 2110−2115.
(18) Sandford, G. Perfluoroheteroaromatic Chemistry: Multifunctional Systems from Perfluorinated Heterocycles by Nucleophilic Aromatic Substitution Processes. In *Halogenated Heterocycles: Synthesis Applications and Environment*; Iskra, J., Ed.; Springer: Berlin, Heidelberg, Germany, 2012; pp 1−31. ISBN 978−3-642−43950−6.
(19) Chambers, R. D.; Hassan, M. A.; Hoskin, P. R.; Kenwright, A.; Richmond, P.; Sandford, G. Polyhalogenated heterocyclic compounds: Part 45. Reactions of perfluoro-(4-isopropylpyridine) with oxygen, nitrogen and carbon nucleophiles. *J. Fluorine Chem.* **2001**, *111*, 135−146.
(20) Romero, N.; Dufrois, Q.; Crespo, N.; Pujol, A.; Vendier, L.; Etienne, M. Regioselective C−F bond activation/C−C bond formation between fluoropyridines and cyclopropyl groups at zirconium. *Organometallics* **2020**, *39* (12), 2245−2256.
(21) Sun, Y.; Sun, H.; Jia, J.; Du, A.; Li, X. Transition-metal-free synthesis of fluorinated arenes from perfluorinated arenes coupled with Grignard reagents. *Organometallics* **2014**, *33*, 1079−1081.
(22) Lu, W.; Gao, J.; Yang, J.-K.; Liu, L.; Zhao, Y.; Wu, H.-C. Regioselective alkyl transfer from phosphonium ylides to functionalized polyfluoroarenes. *Chem. Sci.* **2014**, *5*, 1934−1939.
(23) Zeidan, T. A.; Kovalenko, S. V.; Manoharan, M.; Clark, R. J.; Ghiviriga, I.; Alabugin, I. V. Triplet acetylenes as synthetic equivalents of 1,2-bicarbenes: phantom n,π^* state controls reactivity in triplet photocycloaddition. *J. Am. Chem. Soc.* **2005**, *127*, 4270−4285.
(24) Banks, R. E.; Tsiliopoulos, E. Polymeric analogues of electrophilic fluorinating agents of the N-F class. *J. Fluorine Chem.* **1986**, *34*, 281−285.
(25) Qin, J.; Zhu, S.; Chu, L. Dual photoredox-/palladium-catalyzed cross-electrophile couplings of polyfluoroarenes with aryl halides and triflates. *Organometallics* **2021**, *40* (2021), 2246−2252.
(26) Gutov, A. V.; Rusanov, E. B.; Ryabitskii, A. B.; Chernega, A. N. Octafluoro-4,40-bipyridine and its derivatives: Synthesis, molecular and crystal structure. *J. Fluor. Chem.* **2010**, *131*, 278−281.
(27) Fasina, T. M.; Collings, J. C.; Lydon, D. P.; Albesa-Jove, D.; Batsanov, A. S.; Howard, J. A. K.; Nguyen, P.; Bruce, M.; Scott, A. J.; Clegg, W.; Watt, S. W.; Viney, C.; Marder, T. B. Synthesis, optical properties, crystal structures and phase behaviour of selectively fluorinated 1,4-bis(4'-pyridylethynyl)benzenes, 4-(phenylethynyl)-pyridines and 9,10-bis(4'-pyridylethynyl)-anthracene, and a Zn-(NO3)2coordination polymer. *J. Mater. Chem.* **2004**, *14*, 2395−2404.
(28) Benmansour, H.; Chambers, R. D.; Sandford, G.; Batsanov, A. S.; Howard, J. A. K. Polyhalogenoheterocyclic compounds: Part 54: Suzuki reactions of 2,4,6-tribromo-3,5-difluoropyridine. *J. Fluorine Chem.* **2007**, *128*, 718−722.
(29) Liao, H.-H.; Lee, S.-C.; Kao, H.; Hsu, Y.-L.; Hsu, C.-M.; Tsao, Y.-T.; Miñoza, S.; Li, L.-Y.; Tsai, Z.-N.; Chang, K.-C.; Cheng, C.-K.; Chan, C.-L.; Chien, Y.-S.; Chiu, C.-c. Synthesis of perfluoroaryl sulfides at electron-poor arenes via an S_NAr step with an unexpected mechanism. *Cell Rep. Phys. Sci.* **2022**, *3*, No. 101010.
(30) Rohrbach, S.; Smith, A. J.; Pang, J. H.; Poole, D. L.; Tuttle, T.; Chiba, S.; Murphy, J. A. Concerted nucleophilic aromatic substitution reactions. *Angew. Chem.* **2019**, *58*, 16368−16388.
(31) Lu, J.; Paci, I.; Leitch, D. C. A broadly applicable quantitative relative reactivity model for nucleophilic aromatic substitution (S_NAr) using simple descriptors. *Chem. Sci.* **2022**, *13*, 12681−12695.
(32) Eismeier, S.; Peloquin, A. J.; Stewart, K. A.; Corley, C. A.; Iacono, S. T. Pyridine-functionalized linear and network step-growth fluoropolymers. *J. Fluorine Chem.* **2020**, *238*, No. 109631.
(33) Sheldrick, G. M. Crystal structure refinement with SHELXL. *Acta Cryst. C* **2015**, *71*, 3−8.
(34) Sheldrick, G. M. SHELXT − Integrated space-group and crystal-structure determination. *Acta Cryst. A* **2015**, *71*, 3−8.
(35) Dolomanov, O. V.; Bourhis, L. J.; Gildea, R. J.; Howard, J. A. K.; Puschmann, H. OLEX2: A complete structure solution, refinement and analysis program. *J. Appl. Crystallogr.* **2009**, *42*, 339−341.

https://doi.org/10.1021/acsomega.4c03945
ACS Omega 2024, 9, 28961−28968